Title

Neurofeedback Control in Parkinsonian Patients Using Electrocorticography Signals Accessed Wirelessly With a Chronic, Fully Implanted Device

Journal

IEEE Transactions on Neural Systems and Rehabilitation Engineering, 25(10)

ISSN

1534-4320

Authors

Khanna, Preeya
Swann, Nicole C
de Hemptinne, Coralie
et al.

Publication Date

2017-10-01

DOI

10.1109/tnsre.2016.2597243

Peer reviewed

HHS Public Access

Author manuscript

IEEE Trans Neural Syst Rehabil Eng. Author manuscript; available in PMC 2017 December 27.

Published in final edited form as:

IEEE Trans Neural Syst Rehabil Eng. 2017 October ; 25(10): 1715–1724. doi:10.1109/TNSRE.2016.2597243

Neurofeedback control in Parkinsonian patients using electrocortigraphy signals accessed wirelessly with a chronic, fully implanted device

Preeya Khanna,
UC Berkeley-UCSF Graduate Program in Bioengineering, Berkeley, CA 94703

Nicole C. Swann,
Department of Neurological Surgery, University of California, San Francisco

Coralie de Hemptinne,
Department of Neurological Surgery, University of California, San Francisco

Svjetlana Miocinovic,
Department of Neurological Surgery, University of California, San Francisco

Andrew Miller,
Department of Neurological Surgery, University of California, San Francisco

Philip A. Starr, and
Department of Neurological Surgery, University of California, San Francisco

Jose M. Carmena [Senior IEEE Member]
UC Berkeley-UCSF Graduate Program in Bioengineering, Berkeley, CA 94703

Department of Electrical Engineering and Computer Sciences UC Berkeley and the Helen Wills Neuroscience Institute, UC Berkeley

Abstract

Parkinson's disease (PD) is characterized by motor symptoms such as rigidity and bradykinesia that prevent normal movement. Beta band oscillations (13–30 Hz) in neural local field potentials (LFPs) have been associated with these motor symptoms. Here, three PD patients implanted with a therapeutic deep brain neural stimulator that can also record and wirelessly stream neural data played a neurofeedback game where they modulated their beta band power from sensorimotor cortical areas. Patients' beta band power was streamed in real-time to update the position of a cursor that they tried to drive into a cued target. After playing the game for 1–2 hours each, all three patients exhibited above chance-level performance regardless of subcortical stimulation levels. This study, for the first time, demonstrates using an invasive neural recording system for at-home neurofeedback training. Future work will investigate chronic neurofeedback training as a potentially therapeutic tool for patients with neurological disorders.

Index Terms

Neurofeedback; Parkinson's disease; Brain- computer interfaces

I. Introduction

Neurofeedback refers to the use of real-time acquisition of neural data that is then transformed to extract relevant features and shown to the subject via visual, auditory, or tactile feedback. Previous work has shown that with practice, reinforcement, and feedback, subjects can learn to volitionally control neural activity on the microscale using single neurons [1]–[4], on the mesoscale using brain area-specific local field potentials (LFPs) or electrocorticography (ECoG) signals [5]–[9], and on the macroscale using large cortical network signals measured with electroencephalography (EEG) or functional magnetic resonance imaging (fMRI) [10]–[15].

Using neurofeedback at any of these scales can disrupt or enhance behaviors that rely on the conditioned neural activity. Neurofeedback training has been shown to influence visual perception tasks, motor execution, the incidence of chronic pain, and even seizure frequency in epilepsy patients [4], [7], [12]–[15]. These findings establish neurofeedback as a tool with the potential to first inform how neural signals may be related to a particular behavior, and second be used as a training tool to enable subjects to learn to cognitively control specific, possibly pathological neural activity.

Neurofeedback studies to date either utilize invasive or noninvasive neural recordings. Studies making use of invasive recording systems often require subjects to be in a hospital setting (e.g. [8]) and have not been developed for patients to use while going about their normal daily activities. On the other hand, acquiring non-invasive signals is more convenient but the signal itself suffers from reduced spatial resolution and attenuated high frequency activity, which may be vital for isolating the neural signal of interest. Further, non-invasive systems are sensitive to ambient electronic noise as well as biological artifacts from muscle and eye movements. An ideal neurofeedback system would combine the high signal quality of invasive studies with the convenience of a non-invasive setup. In addition, it would support real-time data streaming and not exert excessive power demands on the device.

The Medtronic Activa PC + S neurostimulator coupled with the Medtronic Nexus-D communication link system enables such capabilities [16]–[18]. This device is an investigational pulse generator capable of delivering continuous constant frequency electrical stimulation, similar to commercially available pulse generators used in DBS for movement disorders such as PD, dystonia, and essential tremor. In addition to delivering therapeutic subcortical stimulation, bipolar ECoG neural signals can also be recorded. Recently, recording invasive cortical ECoG signals chronically has been demonstrated in a nonhuman primate by implanting a quadripolar lead over sensorimotor cortical regions and routing leads (with lead extensions) into the neurostimulator [19]. Coupled with the Nexus-D communication link, the system allows for real-time, wireless transfer of ECoG signals. Here, we leverage the fully embedded, wireless streaming capabilities of the device to investigate whether PD patients can learn to perform a neurofeedback task driven by invasively recorded cortical signals.

We choose to have patients modulate their sensorimotor beta band (13–30 Hz) activity due to its relevance in PD motor symptoms. Many groups hypothesize that a biomarker of

worsened motor symptoms may be related to excessive beta band synchrony in the basal ganglia, and note that dopamine therapy and subcortical deep brain stimulation (DBS) therapy reduce beta band power in these regions [20]–[26]. There is also evidence for changes in motor cortical activity in PD such as increased motor cortico-cortico coherence at 10–35 Hz [27], increased cell synchrony [28], and increased coupling of high frequency (50–200 Hz) amplitude to beta frequency phase [29]. The increased beta synchrony observed throughout the basal ganglia and motor areas may be responsible for impaired computation in primary motor cortex (M1), the final output area in movement generation, potentially resulting in abnormal motor execution in PD.

One strategy for overcoming excessive synchronization of beta frequencies in motor areas may be to reduce M1 beta power. Cortical beta power has been noted to be similar in PD and non-PD patients [29], [30] and in PD patients on DBS or levodopa therapy compared to PD patients off therapy [31]. Despite these baseline similarities, there is evidence of excessive task-related desynchronization of cortical beta power in PD patients during cued movement tasks, interpreted as a compensatory mechanism for reducing abnormal coupling of spiking activity to beta power [30]. Neurofeedback training may be a tool that helps patients develop enhanced cognitive strategies to modulate pathological neural activity, in the same way that some PD patients may have already developed to modulate beta power. Here, we aim to show that PD patients can learn to modulate their cortical beta band signals using a chronically implanted device. Future long-term studies will then quantify effects of beta-band neurofeedback training on PD symptoms.

Each of the three study subjects gained control in the cortical beta band driven neurofeedback task. Though each patient used slightly different combinations of task and device configurations, we show that subjects are able to perform above chance level. One patient exhibited significant learning over the course of a single session of training. To the best of our knowledge, this is the first demonstration of patients performing neurofeedback using a chronically implanted and fully embedded device that can acquire real-time invasive neural signals in a home setting. Efficacy of this system for neurofeedback control could impact not only PD patients, but also patients with other motor and neurological disorders that may benefit from training to modulate pathological neural activity. Furthermore, it paves the way for chronic neurofeedback studies that patients will be able to perform in the comfort of their homes.

II. Materials and methods

A. Consent and Regulatory Approvals

This protocol was approved by the UCSF institutional review board (protocol # 13-10878) under a physician sponsored investigational device exemption (IDE # G120283 to PAS). The study was registered at Clinical Trials.gov (NCT01934296). Informed consent was obtained under the Declaration of the Principles of Helsinki.

B. Patient Characterization and Surgery

Study subjects were evaluated by a movement disorders neurologist and met criteria for a diagnosis of PD (i.e. presence of bradykinesia and at least one other parkinsonian cardinal symptom and responsiveness to levodopa). Baseline motor function in the on medication and off medication states were characterized using the Unified Parkinson's Disease Rating Scale, motor subscale (UPDRS III). Patients were evaluated by a neuropsychologist to exclude significant cognitive impairment or untreated mood disorder.

In all three patients, the 4-contact cortical ECoG lead (Medtroinc model 3587a) was placed in the subdural space through the same burr hole used for the therapeutic subthalamic nucleus (STN) lead. The STN lead was placed with standard methods [32]. At least one contact covered the posterior precentral gyrus (presumed primary motor cortex). Localization of the ECoG strip was confirmed using intraoperative CT merged to the patient's preoperative MRI, as previously described [33]. Then, the free ends of the cortical and subthalamic leads were each connected to 40 cm lead extender (Medtronic model 37087) and tunneled down the neck to a Medtronic Activa PC+S bidirectional neural interface placed in a pocket over the pectoralis muscle. Sessions occurred at 13.5, 11, and 18 months post-surgery for patients 1–3 respectively (see Table I).

C. Contact Selection and Fitting Beta Band Limits

All neural recordings were bipolar. Contact selection occurred prior to the training session using both recorded neural data from previous neural recordings sessions and anatomical location. Contacts that were over sensorimotor areas and exhibited a strong beta desynchronization during overt movement tasks were selected.

For Patients 1 and 3, to estimate the beta band limits to be used for online control, patients performed a 1–2 minute elbow flexion and extension movement in response to quasi-random auditory cues. These tasks elicit strong beta synchronizations and desynchronizations [34]. Using the neural recording during the baseline task, the power spectral density was estimated (see below) in windows of 400 ms at steps of 400 ms (no overlap). The variance of the spectrum at each frequency was plotted. The frequency band in the beta region (10–40 Hz) that yielded the local maxima on the frequency versus variance plot was selected. For Patient 2 a different procedure was used (see *streaming power estimates vs. time domain signals* below)

D. Estimating Beta Power Online

For patient 1, the multi-taper method was used to estimate the baseline spectrum as well as beta power online [6], [7]. In patient 2, however, stimulation was on and due to the low sampling rate, the contaminated signal from the stimulation artifact, and the processor clock artifact (at multiple frequencies, see [35]), the smoothing from the multi-taper method spread artifacts to other frequency band estimates, yielding a noisy estimate of the spectrum. To mitigate this in future patients, time estimates of beta power using the domain signal used a method without smoothing (Welchx02019;s method, pwelch in Matlab).

E. Streaming Power Estimates versus Time Domain Signals

The Activa PC + S accommodates different sampling rates, channel streaming configurations, and filtering options. The sampling rate utilized in this study was 422 Hz (maximum sampling rate supported when devices is streaming data). At this sampling rate, the device can stream one channel of time-domain data per lead (packets of 169 points sent every 400 ms). It can also stream pre-calculated power in a frequency band (2 points sampled at 5 Hz, sent every 400 ms). The benefit of the on-chip power calculation option is that it substantially reduces the battery consumption of the neurostimulator device. In contrast to streaming time-domain data which consumes 2.5 mA, streaming power channels consumes only 90 uA (both estimates in addition to the stimulation current drain of 220 uA) [35]. In order to validate that our experimental paradigm would function in a setting where we used the lower-power on-chip spectral power estimate, we chose to use the on-chip power using beta power calculated from the time-domain channel. Prior work has shown that with stimulation on in the Activa PC+S device, artifacts can be introduced into time domain data and power estimate data at multiple frequencies [35], corrupting the underlying neural signal. In order to avoid the stimulation artifact from compromising beta band recordings, we selected a bandwidth of 15 +/− 2.5 Hz (recommended for a stimulation frequency of 130 Hz) instead of optimizing the beta band frequency limits with the baseline calibration task (as was done for Patients 1, 3).

The Activa PC + S is also outfitted with a number of filter and gain options. Our real-time streamed data was filtered through a low-pass anti-aliasing filter at 260 Hz and a 0.5 Hz high pass filter. We used the maximum gain (2000) that the device allowed. The Activa PC+S also has a data compression feature we used that must be on when streaming data in real-time with Nexus-D.

F. Fitting Beta Power to Cursor Mappings

To fit the mapping between beta power estimates and cursor position, either a simple linear regression (Patients 1, 2) or a Kalman filter (Patient 3) was used. To fit the simple linear regression model, a distribution of baseline beta power estimates from a 1–2 minute movement task was first acquired. The slope and offset of the linear regression was fit using two points ((x_1, y_2) and (x_2, y_2)) where the 25th and 50th percentiles of the beta power distribution from the movement task were x_1 and y_t and the cursor positions at the bottom of the screen and middle of the screen were y_1 and y_2.

The Kalman filter utilized had constant A, W, C, and Q matrices:

$$y_{t+1}=Ay_t+w_t, w_t\sim N(0,W)$$

$$\beta_t=Cy_t+q_t, q_t\sim N(0,Q)$$

where y_t represents cursor position, and β_t represents beta power estimate. C was fit by estimating the target position from the baseline movement task where it was assumed that at all times when beta was in the 0–25th percentile of the overall baseline beta power

distribution, it was aiming to enter the low beta target. Similarly, beta power in the 25th–50th percentile, 50th – 75th percentile, and 75th –100th percentile were assumed to be aiming at the mid-low, mid-high, and high target respectively. Then beta power (β_t) was regressed against these inferred target positions (y_t). Q was calculated as the covariance of ($\beta_t - Cy_t$) where y_t is the inferred target position. A was calculated by adding minimal Gaussian noise to the inferred target position and calculating the correlation between time t and t-1. W was calculated as the covariance of ($y_{t+1} - Ay_t$). Matrices remained constant throughout the task, and the standard time-update and measurement-update steps were utilized to estimate cursor position from neural input and previous cursor state [36].

G. Online Cursor Control

Once a mapping was set, patients began to play the neurofeedback game (see Video 1). The task includes 4 targets each centered at −6, −2, 2, and 6 on a y axis that extends from −10 to 10 (arbitrary units). Targets had a radius of 2 (1.75 in early training for Patient 1 only) and the cursor was a point that was represented by Mario, a popular video game character. The cued target for that particular trial was indicated by the target turning green. Once subjects got their cursor (Mario) in the target, an auditory cue was sounded, and the target turned yellow to indicate success. The score counter on the task interface incremented. Finally, an inter-trial interval time of 1.6 seconds elapsed before the next target was cued (turned green). The GUI and custom code for interfacing with the Activa PC + S using Nexus D and the Medtronic provided Matlab API functions is available on http://github.com/pkhanna104/nexusbmi

H. Assistive Feature

In order to help patients reach targets in early training an ‘assistive feature was used to bring the cursor closer to the final target position that was currently trying to be acquired. The assist was an additive offset to the decoded cursor position:

$$cursor_{pos} = (1 - \alpha) \bullet cursor_{pos,decoded} + \alpha \bullet final_{pos}$$

Where α is a calue between 0 (no assist) and 1 (full assist) that corresponds to how much the assistive feature determines the position of cursor (Fig. 3 for parameters used).

I. Chance Level Calculation

In order to assess performance above chance level of the task, we re-simulated the patient cursor trajectory from late sessions through many task simulations with shuffled target orders. Included in the task simulation is the target and cursor size, hold time, timeout times, and inter-trial intervals. In Fig. 4, we only report counts for those of the four targets that took longer than an average of 2 seconds for patients to acquire.

Due to the variance in the cursor, patients reported that sometimes the middle two targets were acquired before they could pay attention or even recognize that a new target had appeared. In addition, the targets that patients reported as being acquired spuriously had notably faster reaction times (< 2 sec) than other targets. Thus, a mixture of Gaussians analysis was done to see if ‘time to target’ metrics could be better explained by attributing

these quickly acquired targets to a different distribution. First, all ‘time to target’ data across 3 subjects from their late learning sessions (data used in Fig. 4a–c) was pooled.

The mean and standard deviation was estimated for the pooled data, and the resultant probability distribution function was used to calculate the log-likelihood of the data. Then, a second model was fit that used one Gaussian for the quickly acquired targets, and a second Gaussian for the volitionally acquired targets (see Table II for target designation for each patient) and log-likelihood of the data was estimated for the second model. Finally, Akaike information criterion (AIC) and Bayesian information criterion (BIC) were estimated to account for the greater number of parameters in the second model.

The finding that indeed a two-Gaussian distribution better accounted for the ‘time to target’ data than a single distribution, as well as patient reports, caused us to remove the quickly acquired targets in our calculation of patient performance. For example, if the middle two targets were deemed to be spuriously acquired by the previous analysis, and a patient has a final target count of 30 in a particular block, but 15/30 of the simulated targets were trials to the spuriously acquired targets, we would only count the other 15 targets in their final count. Then, if a simulation of the block was performed and the simulation scored 40 targets but 30/40 of the targets are trials to the spuriously acquired targets, we would only count the 10 trials to volitionally acquired targets. Thus, the final count for the actual performance would be 15 and the simulated performance would be 10, in contrast to the original 30 to 40 comparison. Thus, Fig. 4a–c represents performance above chance level for targets that patients had to exert volitional effort to get to.

Note that Patient 1’s chance level calculation (Fig 4a) included blocks where assist was off, whereas Patient 2 chance level included blocks with assist on at a constant level (Fig 4b, c). When the additive assist component was removed from the cursor position trajectory, and the rectified cursor positions were used to calculate chance (as though assist had been off), Patient 2 and 3 still exhibit significantly above chance performance.

J. Statistics

In Fig. 4a–c we report p-values for bootstrapped distributions. Here, p-values represent the percent of simulated task that are greater than actual task performance (one-tailed test). In Fig. 4d–f, the slopes of the linear regression are tested whit a Student’s t-test for significance. In Fig. 5a–f, all beta power data is aggregated and separated by target type (for 4 groups). Each group is z-scored and tested for normality against a standard normal distribution using the Kolmogorov-Smirnov (KS) test. Since at least one group of four fail the KS test at a significance level of 0.05, nonparametric statistics are used for comparisons in Fig 5. The two-tailed Kruskal Wallis test at a significance level of 0.05 was used for tests in Fig. 5a–f, and Fig. 5g–i.

III. Results

Three subjects completed the cortical beta power driven neurofeedback task (Fig. 1). Two subjects visited the UCSF Movement Disorders and Neuromodulation Center, and one patient completed the task at home. All patients had one Activa PC + S device that supports

two quadripolar leads. The lead for DBS therapy was placed in the subthalamic nucleus, while the lead for recording covered sensorimotor cortex. Patients with bilateral therapy also had a separate Activa SC unit (for clinical therapy only). Depending on severity of patient condition, patients were tested either on or off stimulation for the entirety of the neurofeedback training session (Table I). Because ECoG contact locations and the limits of the beta frequency band vary slightly by subject, contact selection and band limits were defined through an initial calibration procedure at the beginning of each patient's training session (see Methods).

After contact selection and beta band frequency limits were selected, a linear mapping between beta band power and the one-dimensional height of a cursor was fit (see Methods). The mapping was fit such that mean beta power during the baseline task positioned the cursor in the middle of the 1D workspace, and beta power above and below baseline levels moved the cursor higher and lower respectively. This position-based mapping is in contrast to many velocity-driven neurofeedback systems.

Patients then proceeded to play a neurofeedback game where they controlled a cursor shaped like Mario, a videogame character from the Nintendo *Mario* franchise, in one dimension by changing their endogenous sensorimotor beta power. On each trial one of the four targets that were uniformly spaced along the 1D workspace was illuminated. Patients' goal was to move the cursor to a position within the illuminated target before the trial timed out (Fig. 1B and Video 1 and 2). Patients completed 5–10 blocks of 5–15 minutes each where they practiced moving the cursor into targets. In early blocks, an assistive feature that moved their cursor closer to the desired target was utilized to make the task easier for patients. As training progressed, the assist was either maintained or reduced (Fig. 3). Patients completed 1–2 hours of training each.

During online control Patients 1 and 3 exhibited beta power peaks that were similar to their baseline recording peak (Fig. 2) illustrated by the match between the beta peak in the power spectral density plot calculated from online control sessions and the horizontal line representing the beta band used for online control (calculated from baseline recordings). Patient 2's baseline beta peck was not used to fit the beta band limits used for online control, which is why the peak in the PSD from online control appears mismatched to the horizontal line illustrating the beta band used for neurofeedback (see Methods for details on Patient 2's beta band fitting procedure).

A. Chance Performance

When examining the average time to target (see Table II), there was a natural division where trials to one or two of the four targets were acquired on average in < 2 sec and trials to the other of the four targets were acquired on average in > 4 seconds. It is possible that the very fast trials were just acquired due to the natural variation of the cursor, in contrast to the patient trying to get the cursor in the target. To determine whether these two groups of 'times to target' were better described by a single distribution or two separate distributions we fit a Gaussian mixture model to the 'time to target' data, and compared the one-Gaussian model to the two-Gaussian model. Using Akaike Information Criterion (AIC) and Bayesian Information Criterion (BIC), we found that times to target were better explained by two

Gaussians (AIC, BIC of one Gaussian: 947.13 and 948.01, and of two Gaussians: 547.06, 548.82). In addition, patients reported that they did not need to control the cursor in order to acquire these easier targets. Because of first, our analysis showing that these times to target are better described by two distributions and second, patients reporting a lack of voluntary control to certain targets, we proceeded to only include the targets with mean acquisition times of > 4 sec in the subsequent chance analyses.

In order to assess whether task performance was above chance level, the cursor trajectory from late training blocks with constant assist level was replayed through a target-shuffled version of the task 1000 times (see Methods). The actual number of successes by each patient was compared to the distribution of successes in simulated performance for targets deemed to be acquired by voluntary control (Fig. 4a–c). Subject performance significantly exceeded the distribution of chance performance (Fig. 4a–c, Patient 1: $p < 0.05$, Patient 2: $p < 0.01$, Patient 3: $p < 0.001$, one-tailed test, Bootstrapped distribution).

B. Task Improvement

Through the course of training, subjects had access to an assistive feature (see Methods for details) that they could use at a level varying between 0 (no assist) to 1 (full assist). Subjects' beta cursor was determined by a linear summation of the cursor position estimated by their neural activity weighted by $1-\alpha$, and the desired target position weighted by α. The assist features thus served to nudge the cursor closer to the cued target. Patients provided verbal input in between blocks indicating what value of α they wanted for the next block. All patients exhibited a trend of reducing or maintaining a constant assist level over blocks indicating that patients felt they were either improving or doing the task proficiently over the course of the session (Fig. 3).

In addition to the reduced reliance on the assist feature, we also analyzed improvement in 'time to target' for late training blocks where patients had a constant assist level. Patient 3 improved significantly in 'time to target' for the mid-low target which was the lowest target achieved by this patient (Fig. 4f). Other patients exhibited non-significant reduction in 'time to target' over the course of late training evidenced by linear regression slopes less than zero (Fig. 4d–e). These improvements are promising but not significant, likely because subjects did too few trials with assist at a constant level.

Interestingly, Patient 1 and 3 exhibited few overt movements during their training sessions, but Patient 2 explored the movement space and converged on a movement strategy (raising his right hand and holding it up) to make their beta power increase. It is possible that he was activating the beta rebound generated post-movement, or persistent beta activity produced during posture maintenance [37]. Discovery of this strategy may have contributed to Patient 2's reduction in time to the highest target whereas Patient 1 and 3 exhibited improvements with mental strategies.

C. Neural Modulation Becomes More Distinct with Training

As subjects relied less on the assist, they learned to generate distinct target-specific neural patterns. We analyzed the beta band input signal preceding target acquisition for each patient from early in the session and late in the session (early: Figs 5a–c, late: Fig 5d–f). Early in

the session patients relied more heavily on the assist feature to move the cursor close to the target, and thus only needed to change their endogenous beta power by a small amount to acquire the target. Thus, the distribution of the beta power produced for each target was not very different. By late in the session though (Fig. 5d–f) subjects learned to generate beta band power at distinct levels: they produced their highest beta power for the highest target, and lowest beta power for the lowest target. Further, late in the session, this target-based separation of beta band power occurs for longer periods of time prior to patients entering the target. Patients 2 and 3 exhibited a significant difference in beta band power at 0.4 seconds (and 0.8 seconds for Patient 2) before their cursor enters the target, compared to early learning where there was no difference (Patient 2: $p < 0.05$ at 0.8 seconds before target acquisition, $p < 0.01$ at 0.4 seconds before target acquisition, Patient 3: $p < 0.01$ at 0.4 seconds before target acquisition, in contrast to no significant differences at these time points in early session data). Overall, patients learned to generate sensorimotor cortical signals containing different amounts of beta power to move the cursor to each of the four targets.

D. Subjects begin to converge broadly on beta band modulation

We investigated how other frequencies co-modulate during the beta power task for the top most and bottom most targets (Fig. 5h–j). We calculated the full power spectrum for trials to the highest target (in red) and trials to the lowest target achieved (lowest beta target in teal for Patients 1, 2 and mid-low target in blue for Patient 3) for late session performance. The spectrum was calculated from the 800 ms prior to the time of target acquisition. Grey rectangles represent significant differences (Kruskal Wallis test, two-tailed, $p < 0.05$).

Patient 1 significantly modulated a large range of frequency values to move the cursor including 6.6 Hz – 26.4 Hz, as well as 38.2 Hz and 52.8 Hz though their control band was only 10–20 Hz. Patient 2 also learned a strategy for modulation covering the large range of 6.6 Hz – 16.5 Hz, and 17.5 Hz – 36.2 Hz although their control band was only 12.5–17.5 Hz. In contrast, Patient 3 modulated only 13.3 Hz – 33.0 Hz and their control band was 20–30 Hz. For all three patients, higher frequencies (< 55 Hz) were not utilized, nor were the lowest frequencies (0.5–5 Hz). Thus patients do not exactly converge on their input beta signal, but they also do not utilize the full spectrum to modulate beta.

IV. DISCUSSION

E. First Demonstration of Neurofeedback Control with a Chronic, Fully embedded Implantable Device Usable At Home

Here we show for the first time to our knowledge use of a chronic, fully embedded implantable device for neurofeedback training in human patients. While neurofeedback paradigms using mesoscale and macroscale neural activity have been demonstrated in humans before, these studies were limited to either one-time invasive recordings with epilepsy patients who were undergoing monitoring for seizures [8], were done with paralyzed patients [38], or were done chronically but in non-human primates [5]–[7]. This paradigm demonstrates the feasibility of chronic neurofeedback training in patients at their homes with an invasive, fully embedded neural recording system accessible without the need

to visit a hospital or clinic (Video 2). This study is a proof of principle for future work on the effects of chronic neurofeedback training utilizing similar implanted devices for access to invasive cortical signals.

Implantable neural devices with better power consumption, artifact rejection, streaming latency, and signal-to-noise ratio (SNR) are in development [39]. All these improvements will further enhance neurofeedback learning by reducing concerns about battery consumption, increasing feedback rate and responsiveness of the system to the patient, and improving the SNR of the desired neural features.

F. Robust Neural Signals in Many Device Configurations

Despite the different device configurations and task parameters used in the three patients (Table 1: beta power extraction method, beta frequency limits, cursor estimation method, stimulation settings, and training session environment), all subjects still performed above chance level. This suggests the cortical beta band signal quality was sufficiently robust to be estimated either by calculating the spectrum from a streamed time-domain signal or a streaming on-chip power estimate. Remarkably, in both cases (streamed time domain or power estimate) the signal was not corrupted by the stimulation signal on the STN lead despite the same device being responsible for generating stimulation and sensing neural data. Further, despite the slow feedback rate (400 ms) in comparison to typical brain-machine interface cursor control studies (<= 100 ms), subjects were still able to process the feedback and use it to update their endogenous beta power.

G. Patients Improve Their Beta Modulation

We had subjects modulate cortical sensorimotor beta band power due to its relevance in PD motor symptoms. Patients exhibited modulation to distinct target-specific beta band power levels (Fig 5d–f), and did so without modulating the entire power spectrum (Fig 5g–i). Patients' best ' time to target' improvement was to different targets (Fig 4d–f) suggesting that target difficulty must vary from patient to patient. This was likely due to variance in baseline beta power calculations which then translated to an offset bias in the beta-to-cursor map fitting. It is of interest that Patient 3 exhibited significant improvement in performance to the lowest beta target (Fig. 4f). Given that literature suggests PD patients may need to compensate for their excessive beta synchrony throughout the basal ganglia and motor areas through earlier and more drastic desynchronizations prior to movement [30], it is perhaps not surprising that Patient 3 learned desynchronization faster. Potentially, practice at desynchronizing aberrant beta activity from normal motor control allowed the patient to exhibit faster improvement to the lower target. Patients 1 and 2 exhibit most improvement in the high beta target (Fig. 4d–e). Patient 2 did find an overt movement strategy that worked for the high target, potentially explaining why improvement was quicker for that target compared to others. Further investigation of synchronization versus desynchronization difficulty can be addressed in longer-term neurofeedback training studies.

H. Limitations

While subjects demonstrate they can learn to increase and decrease cortical beta power, modulating it may not alleviate symptoms. It is possible that changing cortical beta power

will not affect beta synchrony and thus will not affect PD symptoms. It is also possible that the cognitive strategy used to generate or inhibit beta activity is a distinct circuit from the one creating pathological activity.

With respect to the neurostimulator device, streaming time domain neural data for many hours requires substantial battery power. Streaming from the power channel requires less power but still drains the battery [35]. Future systems will use rechargeable batteries eliminating this challenge [39], but current patients implanted without rechargeable batteries may limit their engagement in neurofeedback training to avoid invasive battery replacement surgeries.

I. Future of Neurofeedback as a Therapeutic

While DBS is currently an FDA-approved therapy only for PD, essential tremor, and dystonia, it is being piloted as a therapy for numerous other neurological disorders such as medication-resistant depression, Tourette syndrome, epilepsy, and neuropsychiatric disorders [40]–[43]. For many of these disorders, symptom characterization is more challenging than it is in PD. Exploring neural activity in relevant circuits may shed light on signals that can be used as biomarkers for symptom onset, as well as potential targets for neurofeedback therapy. Since neurofeedback has been shown to be effective at influencing neural signals relevant to specific behaviors [4], [7], [12], [14], it is a promising tool to work in tandem with DBS, with both therapies striving to relieve the patient of pathological neural activity.

Supplementary Material

Refer to Web version on PubMed Central for supplementary material.

Acknowledgments

The authors would like to acknowledge S. Stanslaski, D. Bourget and T. Dension at Medtronic Neuromodulation PLC for technical assistance with interfacing with the Activa PC + S, W. Chen for assistance with clinical sessions, and R. M. Neely for helpful comments on manuscript preparation.

This work was supported in part by the National Science Foundation Graduate Research Fellowship to P.K. and the Defense Advanced Research Projects Agency (W911NF-14-2-0043) to J.M.C.

References

1. Fetz EE. Operant conditionign of cortical unit activity. Science. Feb; 1969 163(3870):955–8. [PubMed: 4974291]
2. Taylor DM, Tillery SIH, Schwartz AB. Direct Cortical Control of 3D Neuroprosthetic Devices. Science. Jun; 2002 296(5574):1829–1832. [PubMed: 12052948]
3. Carmena JM, Lebedev MA, Crist RE, O'Doherty JE, Santucci DM, Dimitrov DF, Patil PG, Henriquez CS, Nicolelis MAL. Learning to Control a Brain-Machine Interface for Reaching and Grasping by Primates. PLOS Biol. Oct.2003 1(2):e42. [PubMed: 14624244]
4. Schafer RJ, Moore T. Selective attention from voluntary control of neurons in prefrontal cortex. Science. Jun; 2011 332(6037):1568–1571. [PubMed: 21617042]
5. Engelhard B, Ozeri N, Israel Z, Bergman H, Vaadia E. Inducing Gamma Oscillations and Precise Spike Synchrony by Operant Conditioning via Brain-Machine Interface. Neuron. Jan; 2013 77(2): 361–375. [PubMed: 23352171]

6. So K, Dangi S, Orsborn AL, Gastpar MC, Carmena JM. Subject-specific modulation of local field potential spectral power during brain-machine interface control in primates. J Neural Eng. Apr.2014 11(2):026002. [PubMed: 24503623]
7. Khanna P, Carmena JM. Changes in reaching reaction times due to volitional modulation of beta oscillations. 2015 7th International IEEE/EMBS Conference on Neural Engineering (NER). 2015:340–343.
8. Schalk G, Miller KJ, Anderson NR, Wilson JA, Smyth MD, Ojemann JG, Moran DW, Wolpaw JR, Leuthardt EC. Two-dimensional movement control using electrocorticographic signals in humans. J Neural Eng. Mar; 2008 5(1):75–84. [PubMed: 18310813]
9. Wang W, Collinger JL, Degenhart AD, Tyler-Kabara EC, Schwartz AB, Moran DW, Weber DJ, Wodlinger B, Vinjamuri RK, Ashmore RC, Kelly JW, Boninger ML. An Electrocorticographic Brain Interface in an Individual with Tetraplegia. PLoS ONE. Feb.2013 8(2):e55344. [PubMed: 23405137]
10. Wolpaw JR, McFarland DJ. Control of a two-dimensional movement signal by a noninvasive brain-computer interface in humans. Proc Natl Acad Sci USA. Dec; 2004 101(51):17849–17854. [PubMed: 15585584]
11. Millan JR, Renkens F, Mourino J, Gerstner W. Noninvasive brain-actuated control of a mobile robot by human EEG. IEEE Trans Biomed Eng. Jun; 2004 51(6):1026–1033. [PubMed: 15188874]
12. Gevensleben H, Holl B, Albrecht B, Schlamp D, Kratz O, Studer P, Wangler S, Rothenberger A, Moll GH, Heinrich H. Distinct EEG effects related to neurofeedback training in children with ADHD: a randomized controlled trial. Int J Psychophysiol. Nov; 2009 74(2):149–157. [PubMed: 19712709]
13. Tan G, Thornby J, Hammond DC, Strehl U, Canady B, Arnemann K, Kaiser DA. Meta-analysis of EEG biofeedback in treating epilepsy. Clin EEG Neurosci. Jul; 2009 40(3):173–179. [PubMed: 19715180]
14. Subramanian L, Hindle JV, Johnston S, Roberts MV, Husain M, Goebel R, Linden D. Real-Time Functional Magnetic Resonance Imaging Neurofeedback for Treatment of Parkinson's Disease. J Neurosci. Nov; 2011 31(45):16309–16317. [PubMed: 22072682]
15. Jensen MP, Gertz KJ, Kupper AE, Braden AL, Howe JD, Hakimian S, Sherlin LH. Steps toward developing an EEG biofeedback treatment for chronic pain. Appl Psychophysiol Biofeedback. Jun; 2013 38(2):101–108. [PubMed: 23532434]
16. Herron J, Denison T, Chizeck HJ. Closed-loop DBS with movement intention. 2015 7th International IEEE/EMBS Conference on Neural Engineering (NER). 2015:844–847.
17. Avestruz AT, Santa W, Carlson D, Jensen R, Stanslaski S, Helfenstine A, Denison T. A 5 W/ Channel Spectral Analysis IC for Chronic Bidirectional Brain #x2013;Machine Interfaces. IEEE J Solid-State Circuits. Dec; 2008 43(12):3006–3024.
18. Stanslaski S, Cong P, Carlson D, Santa W, Jensen R, Molnar G, Marks WJ, Shafquat A, Denison T. An implantable bi-directional brain-machine interface system for chronic neuroprosthesis research. Conf Proc Annu Int Conf IEEE Eng Med Biol Soc IEEE Eng Med Biol Soc Annu Conf. 2009; 2009:5494–5497.
19. Ryapolova-Webb E, Afshar P, Stanslaski S, Denison T, de Hemptinne C, Bankiewicz K, Starr PA. Chronic cortical and electromyographic recordings from a fully implantable device: preclinical experience in anonhumanprimate. J Neural Eng. Feb.2014 11(1):016009. [PubMed: 24445430]
20. Brown P, Mazzone P, Oliviero A, Altibrandi MG, Pilato F, Tonali PA, Di Lazzaro V. Effects of stimulation of the subthalamic area on oscillatory pallidal activity in Parkinson's disease. Exp Neurol. Aug; 2004 188(2):480–490. [PubMed: 15246847]
21. Cassidy M, Mazzone P, Oliviero A, Insola A, Tonali P, Lazzaro VD, Brown P. Movement-related changes in synchronization in the human basal ganglia. Brain. Jun; 2002 125(6):1235–1246. [PubMed: 12023312]
22. Weinberger M, Mahant N, Hutchison WD, Lozano AM, Moro E, Hodaie M, Lang AE, Dosrrovsky JO. Beta oscillatory activity in the subthalamic nucleus and its relation to dopaminergic response in Parkinson's disease. J Neurophysiol. Dec; 2006 96(6):3248–3256. [PubMed: 17005611]

23. Kühn AA, Kupsch A, Schneider GH, Brown P. Reduction in subthalamic 8–35 Hz oscillatory activity correlates with clinical improvement in Parkinson's disease. Eur J Neurosci. Apr; 2006 23(7):1956–1960. [PubMed: 16623853]
24. Kühn AA, Kempf F, Brücke C, Doyle L Gaynor, Martinez-Torres I, Pogosyan A, Trottenberg T, Kupsch A, Schneider G-H, Hariz MI, Vandenberghe W, Nuttin B, Brown P. High-frequency stimulation of the subthalamic nucleus suppresses oscillatory beta activity in patients with Parkinson's disease in parallel with improvement in motor performance. J Neurosci Off J Soc Neurosci. Jun; 2008 28(24):6165–6173.
25. Marsden JF, Limousin-Dowsey P, Ashby P, Pollak P, Brown P. Subthalamic nucleus, sensorimotor cortex and muscle interrelationships in Parkinson's disease. Brain J Neurol. Feb; 2001 124(Pt 2): 378–388.
26. Brown P, Williams D. Basal ganglia local field potential activity: Character and functional significance in the human. Clin Neurophysiol. Nov; 2005 116(11):2510–2519. [PubMed: 16029963]
27. Silberstein P, Pogosyan A, Kühn AA, Hotton G, Tisch S, Kupsch A, Dowsey-Limousin P, Hariz MI, Brown P. Cortico-cortical coupling in Parkinson's disease and its modulation bytherapy. Brain. Jun; 2005 128(6):1277–1291. [PubMed: 15774503]
28. Goldberg JA, Boraud T, Maraton S, Haber SN, Vaadia E, Bergman H. Enhanced synchrony among primary motor cortex neurons in the 1-methyl-4-phenyl-1,2,3,6-tetrahydropyridine primate model of Parkinson's disease. J Neurosci Off J Soc Neurosci. Jun; 2002 22(11):4639–4653.
29. de Hemptinne C, Ryapolova-Webb ES, Air EL, Garcia PA, Miller KJ, Ojemann JG, Ostrem JL, Galifianakis NB, Starr PA. Exaggerated phase-amplitude coupling in the primary motor cortex in Parkinson disease. Proc Natl Acad Sci U S A. Mar; 2013 110(12):4780–4785. [PubMed: 23471992]
30. Rowland NC, De Hemptinne C, Swann NC, Qasim S, Miocinovic S, Ostrem JL, Knight RT, Starr PA. Task-related activity in sensorimotor cortex in Parkinson's disease and essential tremor: changes in beta and gamma bands. Front Hum Neurosci. 2015; 9:512. [PubMed: 26441609]
31. de Hemptinne C, Swann NC, Ostrem JL, Ryapolova-Webb ES, Luciano M San, Galifianakis NB, Starr PA. Therapeutic deep brain stimulation reduces cortical phase-amplitude coupling in Parkinson's disease. Nat Neurosci. Apr.2015 vol advance online publication.
32. Starr PA, Christine CW, Theodosopoulos PV, Lindsey N, Byrd D, Mosley A, Marks WJ. Implantation of deep brain stimulators into the subthalamic nucleus: technical approach and magnetic resonance imaging-verified lead locations. J Neurosurg. Aug; 2002 97(2):370–387. [PubMed: 12186466]
33. Shahlaie K, Larson PS, Starr PA. Intraoperative computed tomography for deep brain stimulation surgery: technique and accuracy assessment. Neurosurgery. Mar; 2011 68(1 Suppl Operative):114–124. discussion 124. [PubMed: 21206322]
34. Crone NE, Miglioretti DL, Gordon B, Sieracki JM, Wilson MT, Uematsu S, Lesser RP. Functional mapping of human sensorimotor cortex with electrocorticographic spectral analysis. I. Alpha and beta event-related desynchronization. Brain J Neurol. Dec; 1998 121(Pt 12):2271–2299.
35. Khanna P, Stanslaski S, Xiao Y, Ahrens T, Bourget D, Swann N, Starr P, Carmena JM, Denison T. Enabling closed-loop neurostimulation research with downloadable firmware upgrades. 2015 IEEE Biomedical Circuits and Systems Conference (BioCAS). 2015:1–6.
36. Wu W, Gao Y, Bienenstock E, Donoghue JP, Black MJ. Bayesian Population Decodin. of Motor Cortical Activity Using a Kalman Filter. Neural Comput. Jan; 2006 18(1):80–118. [PubMed: 16354382]
37. Conway BA, Halliday DM, Farmer SF, Shahani U, Maas P, Weir AI, Rosenberg JR. Synchronization between motor cortex and spinal motoneuronal pool during the performance of a maintained motor task in man. J Physiol. Dec; 1995 489(Pt 3):917–924. [PubMed: 8788955]
38. Hochberg LR, Bacher D, Jarosiewicz B, Masse NY, Simeral JD, Vogel J, Haddadin S, Liu J, Cash SS, van der Smagt P, Donoghue JP. Reach and grasp by people with tetraplegia using a neurally controlled robotic arm. Nature. May; 2012 485(7398):372–375. [PubMed: 22596161]
39. Bourget D, Bink H, Stanslaski S, Linde D, Arnett C, Adamski T, Denison T. An implantable, rechargeable neuromodulation research tool using a distributed interface and algorithm

architecture. 2015 7th International IEEE/EMBS Conference on Neural Engineering (NER). 2015:61–65.

40. Sankar T, Lipsman N, Lozano AM. Deep Brain Stimulation for Disorders of Memory and Cognition. Neurotherapeutics. Jul; 2014 11(3):527–534. [PubMed: 24777384]
41. Morishita T, Fayad SM, Higuchi M, Nestor KA, Foote KD. Deep Brain Stimulation for Treatment-resistant Depression: Systematic Review of Clinical Outcomes. Neurotherapeutics. Jul; 2014 11(3):475–484. [PubMed: 24867326]
42. Laxpati NG, Kasoff WS, Gross RE. Deep Brain Stimulation for the Treatment of Epilepsy: Circuits, Targets, and Trials. Neurotherapeutics. Jul; 2014 11(3):508–526. [PubMed: 24957200]
43. Lyons MK. Deep Brain Stimulation: Current and Future Clinical Applications. Mayo Clin Proc. Jul; 2011 86(7):662–672. [PubMed: 21646303]

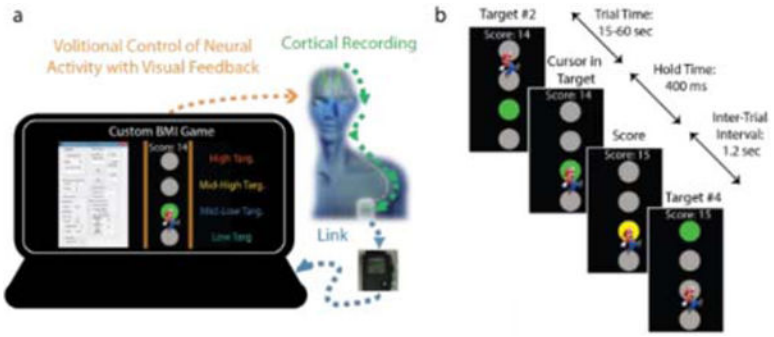

Fig. 1.

System design of neurofeedback task. (A) Patients implanted with the Activa PC + S and cortical leads have the implantable pulse generator located over the pectoralis muscle. A telemetry module has an antenna that sits on the skin surface in close proximity to the IPG and wirelessly acquires neural data and transmits the data to a Windows 7 machine via serial port. The Medtronic Nexus-D application program interface provides functions called from Matlab 2014b to acquire data from the serial port. Neural data is then translated into cursor position. (B) Task timeline begins with a target appearing. The patient then must make the cursor enter the target and hold (in all sessions reported, hold < 400 ms making the hold time effectively 0 ms) after which the target turns yellow and the score count is incremented. An inter-trial interval of 1.6 seconds follows before the next trial begins.

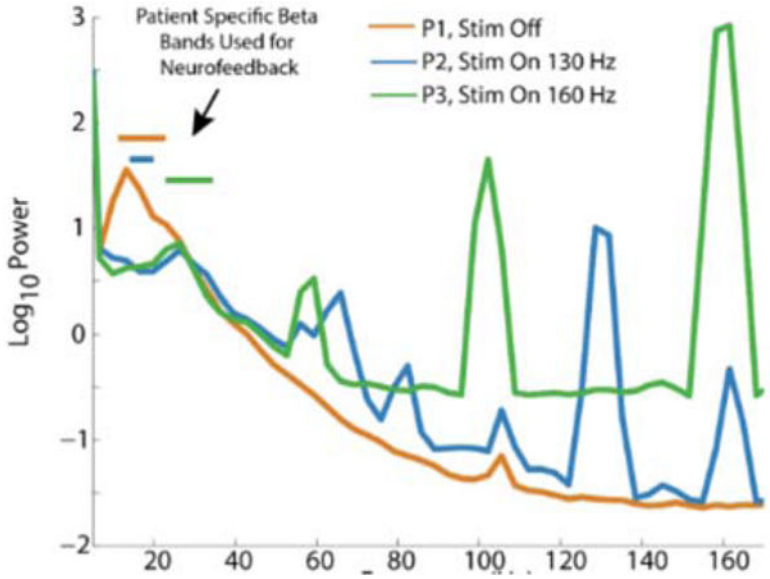

Fig. 2.

Patient power spectral densities during online neurofeedback control. Patient PSDs for cases with stimulation off and stimulation on at 130 Hz or 160 Hz. Despite stimulation, beta peaks are still resolvable. Colored horizontal lines denoted by black arrow show the beta frequency range used for online control for each patient (Patient 1: 10–20 Hz, Patient 2: 12.5–17.5 Hz, Patient 3: 20 – 30 Hz). Note that the beta band used for neurofeedback control in Patient 2 was specially configured for streaming power estimates (instead of time domain data), and does not match the actual beta peak (see Methods)

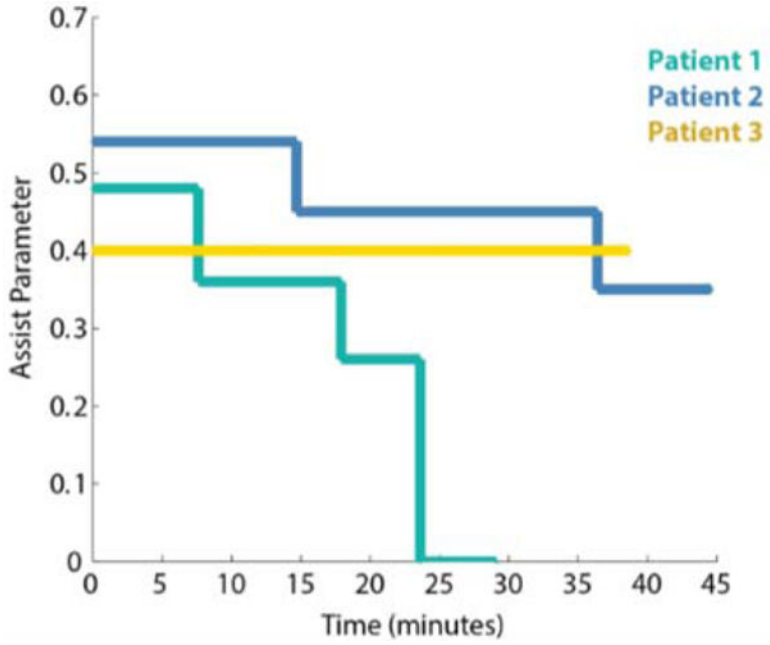

Fig. 3.

Assist parameter used over the course of training for Patients 1–3. Training blocks are concatenated together for visualization, even if time elapsed between blocks. All patients either reduce their reliance on the assist, or maintain a constant assist level throughout the course of training

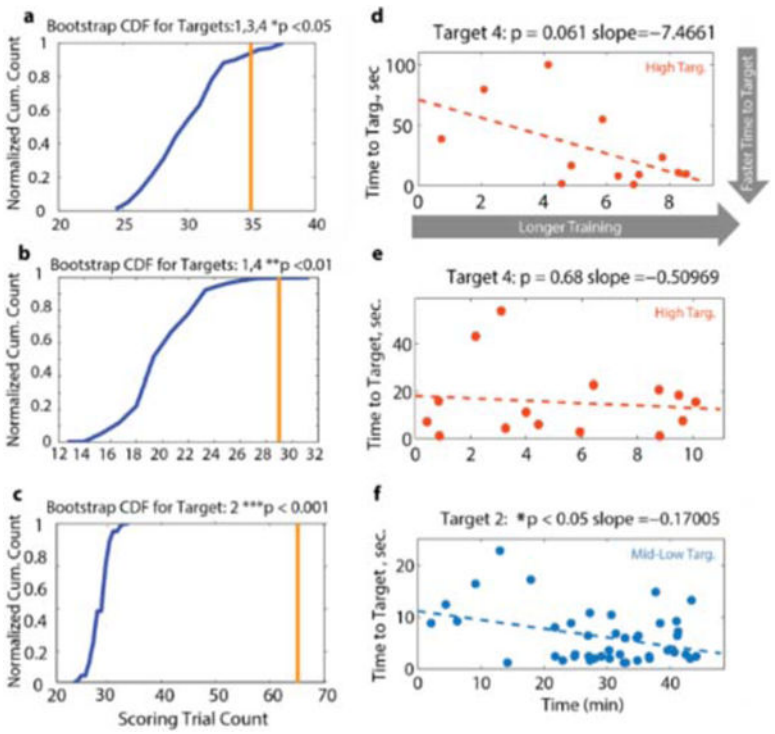

Fig.4.

Patients perform the neurofeedback task above chance levels. (A–C) Patient chance level is illustrated by the blue cumulative distribution (see Experimental Procedures for calculation method). The x axis is total rewards from simulated performance and the y axis is a cumulative normalized count of how many simulations yields that number of rewards. Actual patient performance (total rewards) is shown with the vertical orange line. P-values are printed and are the percent of chance level simulations greater than actual performance (multiplied by two for a two-tailed test). Only data from late learning (constant assist) and from targets with mean time to target greater than four seconds are included in the chance level performance calculation (targets included are denoted in title, see Experimental Procedures). (D–F) For each patient, the time to target is plotted versus session time for the target with most improvement (restricted to late session data) is plotted. Note that for patient 3, the negative slope indicative of reduced time to reach target is sognifocantly different than zero (Student's t-test, $p < 0.05$).

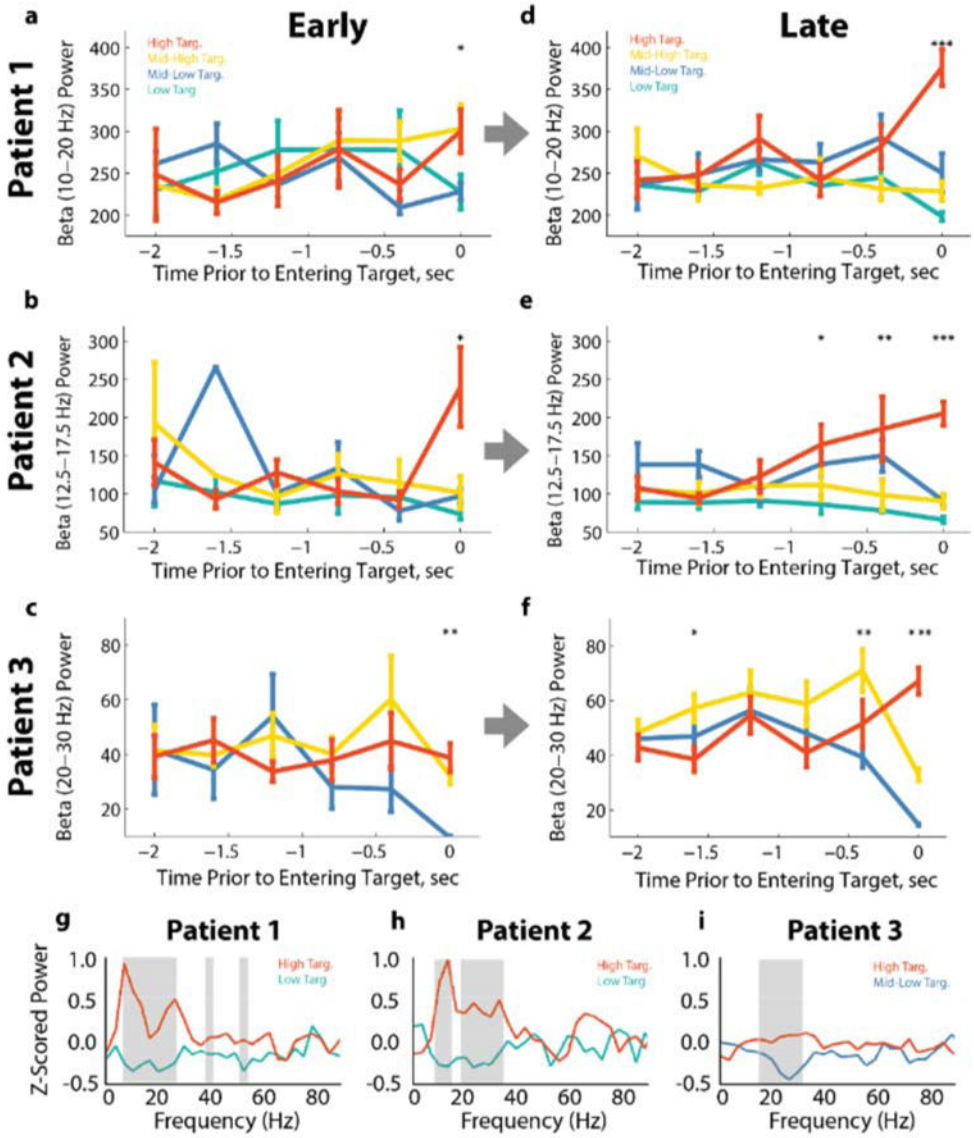

Fig. 5.

Neural changes emerge with training. (A–F) Trial averaged beta power estimates used to drive the cursor are plotted for each patient two seconds before target acquisition to time of targets acquisition (0 sec on x axis). Different traces are for the different targets as indicated by the target color key in (A) and (D). (A–C) show Patient 1–3 neural activity for early in the session (high assist levels). (D–F) show Patient 1–3 neural activity for late in the session (lower constant assist level, same data as Fig 3.). Asterisks indicate significant group differences (Kruskal–Wallis test, * $p < 0.05$, ** $p < 0.01$, *** $p < 0.001$). (G–I) Modulation of full spectrum during neurofeedback task. Traces show trial-averaged z-scored power spectral densities (z-scored by subtracting mean and dividing by standard deviation of aggregated data from late training session) calculated in the 800 ms before target acquisition. Red traces are for the high beta target, teal traces are for the lowest beta target (G, H), and

blue trace is for the mid-low beta target (I). Shaded gray indicates significant difference between the top and bottom target plotted for each subject (Kruskal-Wallis test, $p < 0.05$).

TABLE I

Neurofeedback task parameters for three patients

Patient[#]	Months Post-Surgery	Home or Clinic	Stim On or Off	Stream Time Domain or Power Estimate	Beta Freq. Limits (Hz)	Beta Power Calc Method	Cursor Prediction
1	13.5	Clinic	Off	Time Domain	10–20	Multi-Taper	Linear Reg.
2	11	Home	On	Power Channel	12.5–17.5	On-Chip	Linear Reg.
3	18	Clinic	On	Time Domain	20–30	Welch	Kalman Filter

IEEE Trans Neural Syst Rehabil Eng. Author manuscript; available in PMC 2017 December 27.

Table II

Mean Time to Target (s.d), seconds in Late Training

Patient	Low	Mid-Low	Mid-High	High
1	**5.6 (4.9)**	0.5 (0.3)	**4.0 (4.6)**	**29.3 (32.5)**
2	**20.4 (29.6)**	1.7 (0.9)	1.6 (0.6)	**15.5 (15.3)**
3	n/a	**6.17 (12.6)**	1.34 (0.3)	1.52 (0.2)